

Chiral charge-density wave in TiSe_2 due to photo-induced structural distortions

Darshana Wickramaratne

Center for Computational Materials Science, US Naval Research Laboratory, Washington, D.C. 20375, USA

R. D. Schaller and G. P. Wiederrecht

Center for Nanoscale Materials, Argonne National Laboratory, Lemont, Illinois 60439, USA

G. Karapetrov

Department of Physics, Drexel University, Philadelphia, Pennsylvania 19104, USA

I. I. Mazin

*Department of Physics and Astronomy, George Mason University, Fairfax, VA 22030, USA and
Quantum Science and Engineering Center, George Mason University, Fairfax, VA 22030, USA*

(Dated: October 5, 2020)

A variety of experiments have been carried out to establish the origin of the chiral charge-density wave transition in 1T-TiSe_2 , which in turn has led to contradictory conclusions on the origin of this transition. Some studies suggest the transition is a phonon-driven structural distortion while other studies suggest it is an excitonic insulator phase transition that is accompanied by a lattice distortion. First, we propose these interpretations can be reconciled if one analyzes the available experimental and theoretical data within a formal definition of what constitutes an excitonic insulator as initially proposed by Keldysh and Kopaev. Next, we present pump-probe measurements of circularly polarized optical transitions and first-principles calculations where we highlight the importance of accounting for structural distortions to explain the finite chirality of optical transitions in the CDW phase. We show that at the elevated electronic temperature that occurs upon photoexcitation, there is a non-centrosymmetric structure that is near-degenerate in energy with the centrosymmetric charge density wave structure, which explains the finite chirality of the optical transitions observed in the CDW phase of TiSe_2 .

I. INTRODUCTION

TiSe_2 is claimed to exhibit signatures of two nontrivial phenomena: an excitonic insulator (EI) phase, which is a Bose condensation of excitons, and a chiral charge-density wave (CDW) phase, a state where time reversal symmetry is spontaneously broken [1–10]. This has made it the subject of extensive experimental and theoretical studies, which in turn has led to diverging opinions on the microscopic nature of this transition. Some authors have suggested that the CDW phase of TiSe_2 is mostly due to an excitonic insulator transition and the structural distortion follows this purely electronic transition [1, 11], while other studies have argued that the CDW in TiSe_2 is driven by electron-phonon coupling [8, 12, 13]. A third point of view has suggested that the combination of exciton *and* phonon interactions are required to explain the CDW phase transition [14, 15].

Indeed, some of the experimental and theoretical observations that led to these conclusions don't seem mutually compatible. The plasmon softening [1] and the insulating state observed in photoemission measurements [9] that were associated with the condensation of excitons in the CDW phase can be reproduced with density functional theory (DFT) calculations without invoking the role of excitons [5, 16]. The chirality of the CDW phase [10] is also difficult to reconcile with the fact that the CDW structure is centrosymmetric [3].

These contradictory viewpoints are understandable,

given that there is no distinct symmetry breaking associated with an EI transition that distinguishes it from a structural phase transition. The distinction is solely in the eyes of the beholder. An often discussed litmus test for an EI transition is a *gedanken experiment* where the nuclei are clamped to their equilibrium positions, and the electron subsystem experiences a transition with the atomic coordinates fixed in place. This is an unphysical criterion that neglects the interaction between ions and electrons, which is present in any material. Furthermore, this simplified consideration has a major conceptual problem: it classifies any transition associated with a divergence of the one-electron dielectric response, such as the well-known Peierls transition, as an EI, even though such transitions are not usually described as condensation of excitons.

In this paper we will show that it is possible to reconcile these contradictory viewpoints. Our primary focus will be to provide an explanation for the finite chirality observed in the CDW phase of TiSe_2 and whether this is associated with the condensation of excitons or not. We will do so by presenting a combination of first-principles calculations and optical pump-probe measurements. The article is organized as follows. In Section II we briefly summarize the experimental observations that have led to the conflicting viewpoints mentioned above and propose a working definition for an *exciton condensate* and *chiral charge density wave* that reconciles these phenomena. In Section III we present our own experi-

mental and theoretical results that demonstrate the chiral CDW, which has been observed in optical pump-probe measurements, can be explained by accounting for structural distortions that are screened by the large electronic temperature that occurs in such pump-probe studies. In particular, our working definition of an excitonic insulator (EI) that we present in Section II B and our results in Sec. III shows that (1) the chiral CDW in TiSe_2 is *not* due to a transition to an excitonic insulator phase and (2) the chiral optical transitions observed in pump-probe studies are consistent with a transition of the centrosymmetric ($2 \times 2 \times 2$) structure to a non-centrosymmetric ($2 \times 2 \times 1$) structure, where these two structures are near-degenerate in energy based on our first-principles calculations.

II. GENERAL CONSIDERATIONS

A. Summary of prior experimental studies

Pump-probe optical measurements are often used to address the question of whether the CDW transition is driven by an instability in the electronic or ionic response, since in this experiment one can heat the electron subsystem rapidly, and probe a combination of hot electrons and cold ions. Recently this method was applied to another putative EI, Ta_2NiSe_5 [17], where it was conclusively shown that the gap opening is driven primarily by structural distortions. Numerous attempts to use similar spectroscopic techniques on TiSe_2 [2, 10, 18–20] have also been reported. Time-resolved x-ray diffraction (XRD) measurements or measurements of coherent phonon oscillations [2, 19, 20] performed during these pump-probe studies have shown the structural distortion associated with the CDW can be quenched as a function of increasing laser fluence at lattice temperatures that are well below T_{CDW} . Hence, it was conjectured that since this transition is driven by increasing laser fluence, this purportedly passes the test for TiSe_2 being an EI. Furthermore, plasmon softening [1] has been measured at T_{CDW} and was used as further evidence to support the EI nature of the transition. However, we will show that these assumptions are tenuous.

A phenomenological description of the transient response upon photo-excitation observed in these experiments can be understood as follows. The laser pump excites electrons to a higher energy where the energy is equal to the photon energy of the pump laser. Within a short timescale (femtoseconds) the photoexcited electrons thermalize via electron-electron interactions, which in turn raises the electronic temperature, T_e , of the subsystem while the lattice temperature remains approximately fixed. Increasing the laser fluence raises T_e . Thermalization with the lattice occurs over a relatively longer time scale [21].

The observation of chiral optical transitions at lattice temperatures around or below the CDW transition temperature, T_{CDW} , of 180 K is another piece of intrigue

around TiSe_2 , albeit not directly related with the putative EI physics. In this connection, it was particularly exciting to see several reports of chiral optical transitions [3, 10, 18], *i.e.*, optical transitions with finite circular polarization.

Xu *et al.* [3] observed evidence of a chiral CDW at and below 174 K through measurements of the circular photogalvanic effect (CPGE) current. This finite CPGE signal occurs at a slightly lower temperature than T_{CDW} , which they attributed to a “gyrotropic phase” with a yet-to-be-determined non-centrosymmetric structure that is distinct from the centrosymmetric ($2 \times 2 \times 2$) commensurate CDW phase. The CPGE is a second order nonlinear optical effect that is described by a third-rank tensor that takes on a finite value when inversion symmetry is broken [22]. To first order with respect to an electric field, we will show this is equivalent to the off-diagonal components of the dielectric tensor becoming finite for a hexagonal material such as TiSe_2 . However, one key assumption within the study of Xu *et al.* [3] is that the underlying atomic structure in the CDW phase already has pre-existing chiral domains prior to photoexcitation that make the overall structure chiral. In contrast, we will show that for the case of pump-probe studies performed using high fluence, the CDW structure that is initially centrosymmetric can take on a non-centrosymmetric structure up to a critical value of T_e .

Furthermore, at a critical laser fluence and at a lattice temperature that is below T_{CDW} , the CDW and the finite chirality is quenched [18, 19], which has been interpreted as a non-thermal melting of the CDW phase.

B. What’s in a name?

To interpret these experimental observations, it is instructive to first consider a working definition for these two phenomena; *i.e.*, what is an *excitonic insulator* and what is a *chiral charge density wave*?

When the term *excitonic insulator* [23] was first introduced, it was emphasized that the excitonic insulator is an analogue of BCS superconductivity where the instability occurs in the electron-hole (e-h), rather than the electron-electron (e-e) channel. Within this definition, one would need to invoke higher-order interactions, such as ladder diagrams of the Coulomb interaction to theoretically describe an excitonic insulator phase. These ladder diagrams are not included in standard density functional theory or in its Hartree-Fock like modifications. Hence, the advantage of this definition is that it provides means to directly test whether a material should be classified as an excitonic insulator based on the ability for standard DFT to describe the physical observables associated with such a phase. Note that while any failure of DFT does not imply evidence of an excitonic insulator state, the phenomena associated with an excitonic insulator cannot be described by standard DFT.

For the case of TiSe_2 this includes a simultaneous de-

scription of the $(2 \times 2 \times 2)$ reconstruction of the lattice in the CDW phase, the opening of a gap, the observation of plasmon softening at the CDW transition [1] and non-thermal melting of the CDW in pump-probe measurements at a lattice temperature well below the CDW transition temperature [2, 18, 19]. Hellgren *et al.* [5] used our definition of an excitonic insulator (without explicitly stating this definition) and demonstrated that hybrid functional DFT calculations, which do not incorporate electron-hole ladder diagrams, are able to reproduce the observed $(2 \times 2 \times 2)$ commensurate CDW structure and to describe the insulating state of TiSe_2 .

It is worth noting that another seminal paper [24], which appeared two years after the work of Keldysh and Kopaev, implies that any sort of electronic instability that does not require any lattice degrees of freedom can be classified as an EI. This point of view was adapted in some recent publications [19, 25] to describe an EI phase. We do not find it to be constructive, since this definition would include any and all instabilities associated with a divergence in the plain RPA dielectric function, such as a Peierls transition [26]. Such instabilities predate the notion of an EI by many decades and are not intuitively associated with an EI. Within this interpretation it is assumed that the transition occurs entirely within the electronic subsystem, while the ions follow the electronic CDW. While this line of reasoning may seem compelling, one needs to consider the fact that the ion-ion interaction is screened by electrons, and the response of the electrons may (but does not have to) depend on the electronic temperature, and thus can weaken or eliminate an ionic instability. If this mechanism is operative, the CDW disappears simply because hot electrons in a narrow-gap semiconductor, or in a semimetal, screen better than cold electrons, and therefore suppresses the magnitude of the ion-ion interaction responsible for the instability. Needless to say, this effect is not related to the notion of an excitonic insulator.

Regarding the *chirality* of the CDW phase, a crystal structure is chiral if it can be distinguished from its mirror image; that is, the latter cannot be superimposed onto the original structure by any sequence of rotations or translations [27]. The crystal structure of TiSe_2 is well established [28], and indeed the CDW in a single monolayer of TiSe_2 is chiral, that is, it does not possess a center of inversion and it can formally support magneto-optical effects that need broken time-reversal symmetry. However, the unit cell of the bulk TiSe_2 in both the high temperature phase and the bulk CDW phase is comprised of two monolayers of TiSe_2 stacked alternatively, so that sign of the chirality (“handedness”) alternates and the crystal as a whole is achiral. It is then interesting to note that chiral optical transitions have been associated with this centrosymmetric CDW structure. However, these considerations do not preclude the presence of symmetry-breaking structural distortions of the Ti and/or Se atoms that would lead to a non-centrosymmetric structure.

So, for the purpose of this paper we will define a chi-

ral CDW as a structure that breaks inversion symmetry, and upon including spin-orbit coupling (SOC), leads to a combination of broken inversion and time-reversal symmetry and in turn, non-zero optical chirality. Formally, the observation of finite optical chirality does not have to be necessarily related to breaking of spatial symmetry breaking. For instance, one can imagine, theoretically, a situation when a finite magnetization is generated by optical pumping (even though it is rather unlikely in this material). Obviously — and consistent with the experiment, — in TiSe_2 it is highly unlikely, particularly given that the effect appears only upon heating up the electronic subsystem.

III. RESULTS

A. Pump-probe measurements

We measure the transient change in the reflectivity, R , that is induced by our pump pulse. Our experiments are conducted at 3 K with a pump fluence of 0.17 mJ/cm^2 . The circular dichroism (CD) in transmission geometry is defined as $CD = \frac{A_+ - A_-}{(A_+ + A_-)/2}$ where $A_{+(-)}$ is the absorbance of the right (left) circularly polarized light. However, within the reflection geometry the beam should have no CD signal at normal incidence due to symmetry considerations. However, if the incident beam is at a finite angle from the normal to the sample surface, then circular dichroism in reflection geometry becomes finite. [29]

Measurement of the CD using broadband transient optical reflectivity proceeds by recording the transient change in reflectivity, R , induced by the linearly polarized pump pulse, using a circularly polarized white light probe beam (with right (+) and left (−) handed circular polarization) defined as: $A_{+(-)}(\lambda) = -\lg \frac{R_{\text{pump}}(\lambda)}{R_{\text{no-pump}}(\lambda)}$. The measured transient circular dichroism (TRCD) signal in broadband time-resolved optical reflectivity experiment is then $\Delta R = A_+(\lambda) - A_-(\lambda)$, which corresponds to the degree of circular polarization. We identify two different relaxation time scales for the TRCD: a picosecond time scale which is commensurate with electron-phonon relaxation times and a longer nanosecond timescale that is typically associated with phonon-phonon relaxation times. Figure 1 illustrates the wavelength dependence of the optical density due to left and right circularly polarized light measured on the picosecond time scale and the circular dichroism as a function of wavelength.

At 3 K (well below $T_{\text{CDW}} \sim 180 \text{ K}$), we find the degree of circular polarization is finite in the spectral range between $\lambda=550 \text{ nm}$ and $\lambda=725 \text{ nm}$. We also find the degree of circular polarization to be finite in this wavelength range for TRCD measured on the nanosecond timescale [30]. Further details on these two relaxation time scales and the approach used to extract these decay times from the raw transient reflectivity data are con-

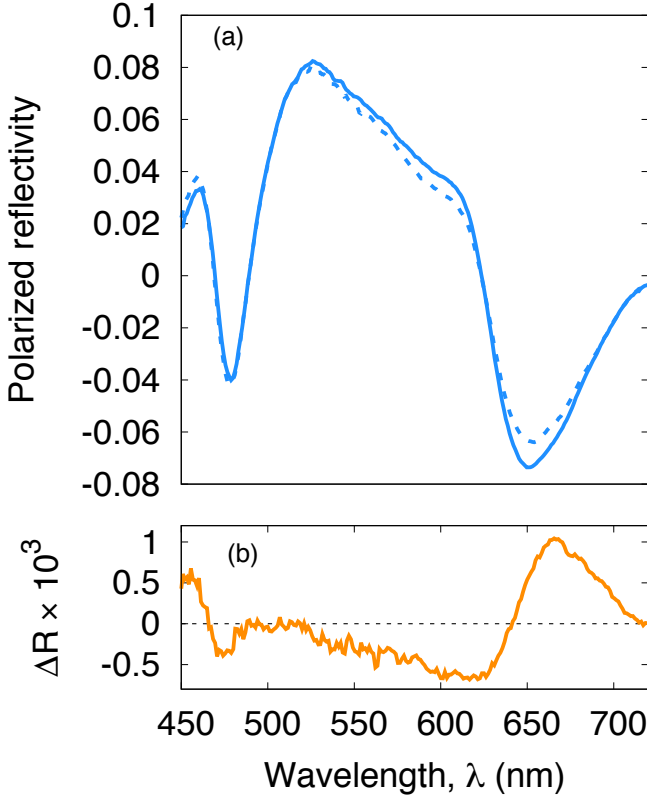


FIG. 1: (a) Change in the right handed (solid line) and left hand (dotted line) transient reflectivity obtained on picosecond time scales as a function of wavelength. (b) Difference between the right and left handed transient reflectivity, ΔR , which is the degree of circular polarization.

tained in Ref. 18. Our results, in agreement with Ref. [19], shows that above the critical fluence we use in this study, the chirality of the optical transitions is zero and the chiral CDW is quenched.

As we discuss in Sec. II, the pump pulse used in our study will lead to a change in the electronic temperature T_e of the system while the lattice temperature remains fixed. Let us estimate what value of T_e this corresponds to. For a given photon fluence, P , material volume, V , penetration depth of the excitation, l , electronic specific heat for formula unit, C_e and the magnitude of the reflectivity, R , the critical electronic temperature is defined as $T_e = (1 - R)PV/(lC_e)$. The electronic specific heat, C_e , is defined as: $C_e = \frac{\pi^2}{3}NT_e$, where N is the average electronic density of states per formula unit. The average electronic specific heat, C , when the TiSe₂ carriers are heated from an electronic temperature of 0 K to T_0 K can be defined as $\frac{\pi^2}{3}N \int_0^{T_0} TdT = \frac{\pi^2 T_0}{6}$. Hence, $T_e = 6(1 - R)PV/l\pi^2$. In our experiment we use an excitation wavelength, λ , of 800 nm. The absorption index at this wavelength is ~ 3.2 [31, 32]. Combining this information, we determine the penetration depth, l as $\lambda/(4\pi\kappa)$ and obtain a value of $l \sim 19$ nm. The fluence, P , used for the results report in Fig. 1 is 0.17 mJ/cm². Using

the density of states at the Fermi level of ~ 1 state/eV per formula unit, from our first-principles calculation, we find $C_e \sim 2.36T_e$. The volume of the TiSe₂ unit cell is 0.072 nm³ and the reflectivity, R at $\lambda=800$ nm is ~ 0.5 [33].

Combining all of this information leads to a $T_e \sim 690$ K. Note that other studies have reported different values of fluence and a slightly different λ of 790 nm at which the CDW is suppressed. The values for the critical fluence, P , ranges between 0.17 mJ/cm² to 0.5 mJ/cm² [2, 18, 19]. This leads to a range of values for T_e , the lowest value being ~ 690 K and the highest value is ~ 1180 K.

The experimental data above shows that TiSe₂ exhibits a finite chirality in the optical reflectivity with the peak in the chirality centered at ~ 625 nm. The lattice temperature for these measurements is 3 K while the electronic temperature at the fluence used in Fig. 1 corresponds to T_e of 690 K. As we discuss in Sec. II at a lattice temperature of 3 K, TiSe₂ is expected to take on the centrosymmetric $P\bar{3}c1$ structure which should not lead to finite chirality. In the following we aim to rationalize this puzzling observation by performing first-principles calculations based on density functional theory (DFT).

B. DFT calculations

Above the CDW transition temperature, bulk 1T-TiSe₂ is stable in a hexagonal centrosymmetric structure (space group 164, $P\bar{3}m1$) where the Ti atoms are octahedrally coordinated by Se. We use the experimental lattice constants of bulk TiSe₂ in the normal phase ($a=3.527\text{\AA}$ and $c=5.994\text{\AA}$) [28] to determine the electronic structure. We find the high- T phase to be a semi-metal, with a hole-like pocket at Γ and an electron-like pocket at M and L, in agreement with previous calculations of the bulk structure of TiSe₂ [5]. The hole pocket at Γ is derived primarily from Se p_z states, while the electron pockets are derived from Ti d -states.

The CDW transition temperature, T_{CDW} , of bulk TiSe₂ is ~ 180 K [28, 34], below which TiSe₂ undergoes a $(2 \times 2 \times 2)$ reconstruction to the commensurate CDW phase. This is accompanied by a displacement of the Ti along the basal plane and a minor rotation of the Se atoms around each Ti atom, [28] and the corresponding space group of the structure changes from $P\bar{3}m1$ to $P\bar{3}c1$. Recent studies [35, 36] have also suggested that displacements of the Ti and Se atoms that are distinct from the $P\bar{3}c1$ structure. Within our DFT calculations, we find each of these displacement patterns of the Ti and Se atoms within the $(2 \times 2 \times 2)$ reconstruction to be near degenerate in energy with respect to each other. More importantly, all these structures are centrosymmetric, similar to the $P\bar{3}m1$ unreconstructed structure or the $P\bar{3}c1$ CDW structure.

As we discuss in Sec. II, a structural distortion that leads to a non-centrosymmetric structure may be a plausible source of the finite optical chirality that has been

observed in the CDW phase. If we examine the calculated phonon dispersion for TiSe_2 [5], we note that there are two soft modes, one at the M and a second at the L high-symmetry points, which correspond to structural instabilities. Indeed, the soft mode at the L-point corresponds to the $(2 \times 2 \times 2)$ CDW reconstruction. The soft mode at the M-point would correspond to a $(2 \times 2 \times 1)$ structural distortion. Such a structure, which has a lower space group, $P321$, does not possess a center of inversion. Figure 2 illustrates these two possible structural distortions that can occur starting from the high-temperature $P\bar{3}m1$ structure.

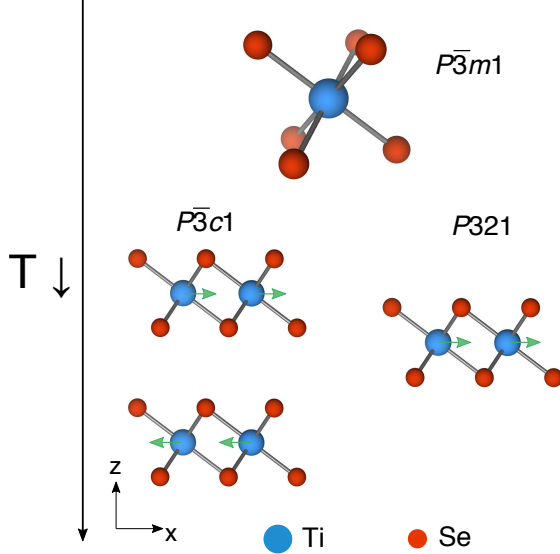


FIG. 2: Schematic depiction of how the achiral centrosymmetric high temperature $P\bar{3}m1$ structure can transform into either the achiral centrosymmetric $P\bar{3}c1$ CDW structure or the chiral non-centrosymmetric $P321$ CDW structure as the temperature, T , is lowered below the CDW transition temperature. The green arrows indicate the direction that the Ti atoms are displaced in the CDW phase.

In order to elucidate whether these structural distortions are impacted by the elevated electronic temperatures that occur in pump-probe studies, we performed DFT calculations, varying the magnitude of the electronic temperature, $\sigma = kT_e$ from 0.005 eV to 0.1 eV (corresponding to an effective T_e of ~ 58 K to ~ 1160 K) and optimize the atomic coordinates of TiSe_2 using both $(2 \times 2 \times 1)$ and $(2 \times 2 \times 2)$ reconstructions. Within this approach we assume the photoexcited electrons in our pump-probe study have thermalized (within femtoseconds as discussed in Sec. II) to an electronic temperature that is determined in part by the fluence while the lattice temperature remains fixed.

In practice, this is done by varying the magnitude of the Fermi-Dirac energy broadening, σ , used in the self-consistent cycle of our DFT calculations (cf. Sec. V and Ref. 30). For each value of σ , we perform a structural optimization and determine the distance, δ_{Ti} , by which the Ti atoms are displaced away from their high-symmetry positions within the $P\bar{3}m1$ structure.

In agreement with published results [5], we find the $(2 \times 2 \times 2)$ to be the ground state, and the magnitude of the displacement, δ_{Ti} , to be somewhat underestimated (it was shown in Ref. [5] that this may be corrected by adding a small fraction of Hartree-Fock exchange using a hybrid functional). The normalized displacements with respect to the displacement determined for the lowest energy broadening ($\sigma = 0.005$ eV, $T_e = 58$ K), δ_0 , are shown in Fig. 3 for the $P321$ structure.

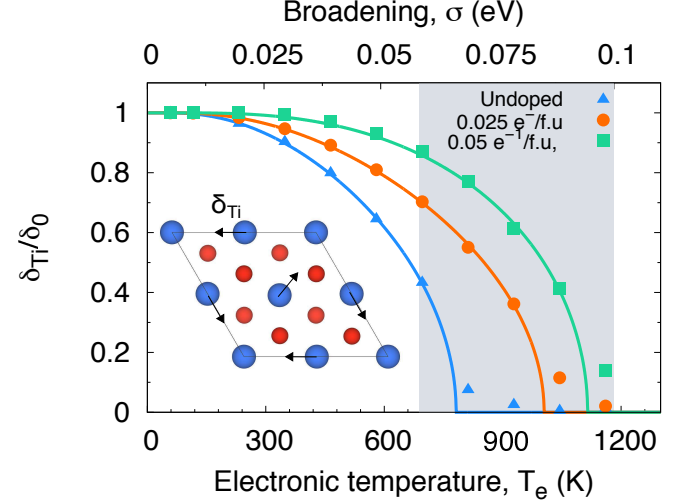


FIG. 3: Normalized displacement of the Ti atoms in the $P321$ structure as a function of the magnitude of the broadening, σ , and corresponding electronic temperature, T_e . Results for an undoped (blue - Δ), and doping with $0.025 e^-/\text{f.u.}$ (orange - \circ) and $0.05 e^-/\text{f.u.}$ (green - \square) are illustrated. The solid lines are a fit to Eq. 1. The critical temperature, T_c where the structure transforms to $P\bar{3}m1$ from $P321$ is the value of T_e when the solid line intersects the horizontal axis for each fit. The range of critical electronic temperatures where the chirality of the CDW is found to be suppressed in pump-probe experiments is illustrated with the grey shaded rectangle. A top view of the $P321$ structure is illustrated in the inset with the arrows illustrating the direction the Ti atoms are displaced.

We find that for low values of σ , the Ti atoms are displaced strongly away from their corresponding high-symmetry position and the structure retains the low-symmetry $P321$ structure. However, at a critical value of the electronic temperature, $T_e = T_c$, the Ti atoms converge to their high-symmetry positions and the structure is stable in the undistorted $P\bar{3}m1$ structure. We plot $\delta_{\text{Ti}}/\delta_0$, which we define as the order parameter for this structural transition as a function T_e and find that it exhibits a BCS-like temperature dependence. If we fit our first-principles calculations in Fig. 3 to the following BCS expression

$$\frac{\delta(T)}{\delta_0} = \tanh \left(b \sqrt{\frac{1}{T} - 1} \right) \quad (1)$$

we find a critical temperature, T_c , to be 782 K, at which

the non-centrosymmetric $P321$ structure transforms to the high-temperature centrosymmetric $P\bar{3}m1$ structure (with a Hartree-Fock correction added as in Ref. [5], this temperature would likely be slightly higher).

We also consider the effect that intrinsic doping may have on this structural phase boundary. Several studies have shown as-grown TiSe_2 exhibits n -type conductivity that is likely due to unintentional impurities or native defects [37–39], which act as a source of excess electrons. To this end, we simulate the effect of n -type doping by changing the number of valence electrons and adding a compensating jellium background charge, and optimize the atomic coordinates and the volume starting from the $P321$ structure for different values of σ . We investigate the effect of the following doping concentrations; $0.025 e^-/\text{TiSe}_2$ f.u., $0.05 e^-/\text{TiSe}_2$ f.u. The change in $\delta_{\text{Ti}}/\delta_0$ as a function of σ with respect to doping is also illustrated in Fig. 3. We fit the results of $\frac{\delta_{\text{Ti}}}{\delta_0}$ for the two different doping levels to Eq. 1 and find T_c increases to 1005 K for $0.025 e^-/\text{TiSe}_2$ f.u. and T_c is 1115 K for a doping concentration of $0.05 e^-/\text{TiSe}_2$ f.u.

We also conducted a similar analyses as in Fig. 3, taking into account different approximations within DFT [30] and find qualitatively similar behavior. The order parameter always exhibits a similar BCS-like temperature dependence and the T_c obtained by fitting $\frac{\delta_{\text{Ti}}}{\delta_0}$ versus T_e to Eq. 1 for the different approximations we tested is within 6% of the T_c for undoped TiSe_2 reported in Fig. 3.

Applying the same procedure to the centrosymmetric $P\bar{3}c1$ CDW structure, we find it also converges to the $P\bar{3}m1$ structure at large values of T_e . This is reflected in our calculations of the difference in the total energy of the $P321$ and $P\bar{3}c1$ structures with respect to $P\bar{3}m1$ structure as a function of T_e , as illustrated in Fig. 4. Note that while the $P\bar{3}c1$ structure is slightly lower in energy than the $P321$ structure for all values of σ , in agreement with the static equilibrium structure. This difference in energies is very small and may be reversed at some value of T_e , once the effects of vibrational entropy are properly accounted for. We speculate, based on our experimental findings, that this happens at some electronic temperature, T_1 , such that $0 < T_1 < T_c$.

Hence, from these calculations the following picture emerges. While the centrosymmetric $P\bar{3}c1$ structure is the ground state CDW phase, the non-centrosymmetric $P321$ structure is near-degenerate in energy. Hence, upon photo-excitation, the rapid increase in T_e stabilizes the $P321$ structure when T_e becomes larger than T_1 , and the magnitude of the displacement of the Ti atoms with respect to the $P\bar{3}m1$ structure depends on T_e . The $P321$ structure lacks a center of inversion and this, as we will show in Section III C, leads to finite circular dichroism, *i.e.*, a chiral CDW. When T_e increases due to increasing fluence, the Ti atoms are weakly displaced with respect to their positions within the $P\bar{3}m1$ structure. At $T > T_c$, the ion-electron interactions are sufficiently weak so that the transition to the non-centrosymmetric $P321$, or the centrosymmetric $P\bar{3}c1$ structure no longer occurs.

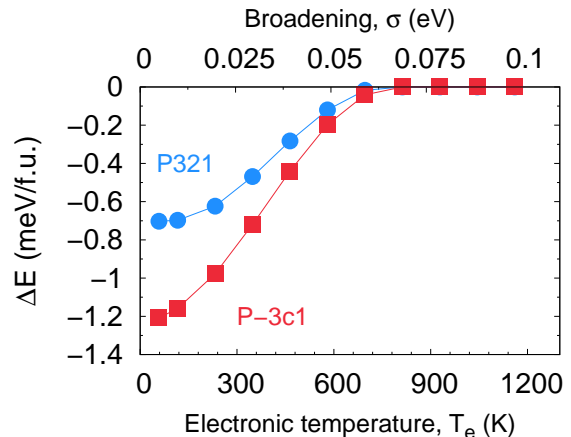


FIG. 4: Change in total energy of the two CDW structures, achiral $P\bar{3}c1$ (\square) and chiral $P321$ (\circ) with respect to the total energy of the high-temperature $P\bar{3}m1$ structure as a function of the electronic temperature.

Instead, the achiral centrosymmetric $P\bar{3}m1$ structure is stable and the finite circular polarization is quenched, *i.e.* non-thermal melting of the (chiral) CDW occurs.

Our estimate for the critical electronic temperature, T_c , from our first-principles calculations, where the chiral $P321$ structure is quenched ranges between 730 K for undoped TiSe_2 up to 1115 K for TiSe_2 doped with $0.05 e^-/\text{TiSe}_2$ f.u., which is well within the range of values for the critical T_e that we estimate by analyzing pump-probe experiments at the end of Sec. III A. This proves that the suppression of the optical chirality as a function of increasing laser fluence observed in pump-probe studies is not related to the presence of an excitonic insulator. Instead it is due to structural distortions that are screened by an elevated electronic temperature.

C. Optical properties

To demonstrate that the centrosymmetric $P\bar{3}c1$ and the noncentrosymmetric $P321$ structures do indeed lead to zero and non-zero chirality in their optical transitions, respectively, we calculate the real and imaginary parts of the dielectric function. We then determine the reflectivity, R , and the degree of chirality, η [30]. The calculated reflectivity is illustrated in Fig. 5.

First, we find the magnitude of the total reflectivity does not vary significantly for either the $P\bar{3}c1$ or the $P321$ CDW structures or the high-temperature $P\bar{3}m1$ structure. For photon energies between 0.5 eV and 2.5 eV the magnitude of the reflectivity ranges between ~ 0.4 and ~ 0.6 . The reflectivity for the $P321$ structure is illustrated in Fig. 5. We note that magnitude of the reflectivity across this range of energies is also consistent with what has been measured experimentally [33].

To determine the degree of circular dichroism of the reflectivity we then compare the difference between the

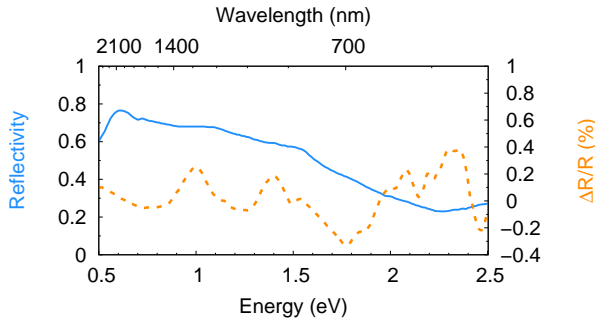


FIG. 5: Reflectivity as a function of photon energy (blue solid line - left vertical axis) and the degree of circular polarization associated with these optical transitions (orange dotted line - right vertical axis) calculated for the non-centrosymmetric $P321$ structure.

off-diagonal components of the imaginary part of the dielectric function [30]. Since the high temperature $P\bar{3}m1$ structure and the $P\bar{3}c1$ CDW structure both possess a center of inversion and they also preserve time-reversal symmetry, left and right circularly polarized optical transitions are equal in magnitude and, as a result, one would expect the degree of circular dichroism to be zero. Indeed, we find this to be the case from our first-principles calculations for the two centrosymmetric structures, i.e. they are achiral.

However, for the non-centrosymmetric $P321$ structure, we find the off-diagonal components of the dielectric function are finite and this leads to finite circular polarization as we show in Fig. 5. The degree of circular polarization is finite within an energy range of 1.5 eV to 2 eV, which is approximately the energy range where finite circularly polarized transitions occurs in our pump-probe measurements of TiSe_2 (Fig. 1(b)). This is also consistent with the range of wavelengths where finite circular polarization has been observed in previous pump-probe studies of TiSe_2 [2, 19]. We also conjecture that continuous wave excitation under sufficiently high power, long duration and at lattice temperatures below T_{CDW} , as used in the study by Xu *et al.* [3], may also conspire to lead to the finite CPGE current. Based on our results and discussion presented above, this does not require the pre-existence of chiral domains. Instead, photoexcitation above a critical power may lead to a finite fraction of the atomic structure to be trapped in the non-centrosymmetric $P321$ structure, which would lead to finite chirality.

Hence, from these calculations we can conclude the following. The observation of chiral optical transitions during pump-probe measurements on TiSe_2 cannot be explained by the conventional $P\bar{3}c1$ structure that is associated with the $(2 \times 2 \times 2)$ commensurate CDW phase of TiSe_2 . Instead, a symmetry breaking mechanism that leads to a finite difference between right and left circularly polarized optical transitions has to be operative. Our calculations suggest the non-centrosymmetric $P321$ structure that is near-degenerate in energy with the $P\bar{3}c1$

is stabilized upon photo-excitation. The $P321$ structure leads to finite circularly polarized transitions that are consistent with the signatures of the chiral CDW that have been identified in pump-probe studies of TiSe_2 .

IV. CONCLUSIONS

Comparing our first-principles calculations with experiment, we draw two main conclusions. First, the experimentally observed non-thermal melting of the CDW in TiSe_2 , that is, melting of the CDW upon heating the electron subsystem, can be quantitatively explained by the effect of the electronic temperature on the electron screening of the ion-ion interactions. This is a one-electron effect not related in any manner with the physics of excitonic insulators. Therefore, non-thermal melting of the CDW alone does not provide evidence for the existence of an excitonic insulator state in TiSe_2 .

Second, we observe, in agreement with previous measurements, that the chiral optical response of TiSe_2 exists for a finite range of laser fluences, in other words, within a finite range of electronic temperatures. To this effect, we calculated the energy difference between the ground state centrosymmetric CDW structure ($P\bar{3}c1$) and the non-centrosymmetric $P321$ CDW structure, and found it to be extremely small (~ 10 K). Furthermore, this energy difference rapidly decreases as the electronic temperature increases. We conjecture that there is a small additional energy term, possibly related to vibrational entropy, that is outside the scope of our static lattice DFT calculations, which is either independent of the electronic temperature, or even grows with it. Such a contribution would impact the energy difference between the $P321$ and $P\bar{3}c1$ structures and lead to the noncentrosymmetric $P321$ structure to be the ground state at some intermediate electronic temperature, T_1 .

V. METHODS

A. Experiments

Single crystals of TiSe_2 were prepared using the chemical vapor transport technique with iodine as a transport agent in a manner similar to that used by Oglesby *et al.* [40]. We used Titanium powder (99.99%), Selenium powder (99.999%), and Iodine powder (99.99%) purchased from Alfa Aesar. The powders were premixed and inserted into quartz tubes which were evacuated to 10^{-4} mTorr. We allowed crystal growth to proceed for 3 weeks before quenching the reaction and retrieving the single crystals.

Broadband transient optical reflectivity was measured using the split output of an 800 nm 35 fs Ti:sapphire laser system equipped with an optical parametric amplifier. The pump pulses, having a wavelength of 800 nm (1.55 eV), were incident on the sample at 1 kHz using

a synchronized chopper that blocks every other pulse of the parent laser operating at a 2 kHz repetition rate. A delayed white light supercontinuum probe was generated by focusing the 800 nm laser into a CaF_2 plate. The pulse beam had a 600 μm diameter spot size and the probe beam spot size had a 100 μm diameter. An adjustable time delay is established between the pump and probe pulse by means of a mechanical track that adjusts the path of the probe pulse. The pump beam was incident on the sample at an angle of incidence close to 20° and the probe beam was oriented with an angle of incidence at 30° . The pump pulse is linearly polarized while the probe pulse is circularly polarized (CP). In order to control the handedness of the CP probe beam a Pockels cell was inserted into the probe beam path. The Pockels cell using a KD^*P crystal was driven using the low jitter Q-switch driver QBU-BT-6024-LJ from Vigitek, Inc. (<http://vigitek.biz>). All of the pump-probe data was obtained at 3 K (well below $T_{\text{CDW}} = 200$ K) with a pump fluence of 0.17 mJ/cm².

B. First-principles calculations

Our calculations are based on density functional theory within the projector-augmented wave method [41] as implemented in the Vienna *Ab-initio* Simulation Package (VASP) [42, 43]. All of the results in the main text use the generalized gradient approximation (GGA) defined by the Perdew-Burke-Ernzerhof functional [44]. We use the Ti PAWs where the 3*d*, 4*s*, 4*p* and the Se PAWs where the 4*s*, 4*p* electrons are treated as valence and a plane-wave energy cutoff of 400 eV. All of the structural relaxations of the bulk unit cell used a $(24 \times 24 \times 12)$ *k*-point grid. Calculations of the $(2 \times 2 \times 2)$ and the $(2 \times 2 \times 1)$ CDW structures used *k*-point grids that were scaled with respect to the *k*-point grid used for the unit cell. An energy convergence criteria of 10^{-8} eV and a force convergence criteria of 2 meV/ \AA was used for all of the calculations. To examine the structural phase transition as a function of electronic temperature we used the Fermi-Dirac smearing scheme. The Grimme-D3 correction scheme was used to account for van-der-Waals interactions [45]. The space groups of the different structures were determined using spglib [46]. To determine the circular polarization of the optical transitions, we calculate the imaginary and real part of the dielectric function with spin-orbit interaction included.

VI. DATA AVAILABILITY

The data that support the findings of this study are available from the corresponding author upon reasonable request.

Acknowledgments

We thank Nuh Gedik, Qiong Ma, and Su-Yang Xu for insightful discussions. D.W. was supported by the Laboratory-University Collaboration Initiative of the DoD Basic Research Office. G.K acknowledges support from the NSF under Grant No. ECCS-1711015. Use of the Center for Nanoscale Materials, an Office of Science user facility, was supported by the U.S. Department of Energy, Office of Science, Office of Basic Energy Sciences, under Contract No. DE-AC02-06CH11357. I.I.M. was supported by ONR through grant N00014-20-1-2345.

-
- [1] A. Kogar, M. S. Rak, S. Vig, A. A. Husain, F. Flicker, Y. I. Joe, L. Venema, G. J. MacDougall, T. C. Chiang, E. Fradkin, et al., *Science* **358**, 1314 (2017).
- [2] T. Rohwer, S. Hellmann, M. Wiesenmayer, C. Sohrt, A. Stange, B. Slomski, A. Carr, Y. Liu, L. M. Avila, M. Kalläne, et al., *Nature* **471**, 490 (2011).
- [3] S.-Y. Xu, Q. Ma, Y. Gao, A. Kogar, A. Zong, A. M. M. Valdivia, T. H. Dinh, S.-M. Huang, B. Singh, C.-H. Hsu, et al., *Nature* **578**, 545 (2020).
- [4] J. van Wezel, *EPL* **96**, 67011 (2011).
- [5] M. Hellgren, J. Baima, R. Bianco, M. Calandra, F. Mauri, and L. Wirtz, *Phys. Rev. Lett.* **119**, 176401 (2017).
- [6] F. Weber, S. Rosenkranz, J.-P. Castellán, R. Osborn, G. Karapetrov, R. Hott, R. Heid, K.-P. Bohnen, and A. Alatas, *Phys. Rev. Lett.* **107**, 266401 (2011).
- [7] T. Kidd, T. Miller, M. Chou, and T.-C. Chiang, *Phys. Rev. Lett.* **88**, 226402 (2002).
- [8] K. Rossnagel, L. Kipp, and M. Skibowski, *Phys. Rev. B* **65**, 235101 (2002).
- [9] H. Cercellier, C. Monney, F. Clerc, C. Battaglia, L. Despont, M. Garnier, H. Beck, P. Aebi, L. Patthey, H. Berger, et al., *Phys. Rev. Lett.* **99**, 146403 (2007).
- [10] J. Ishioka, Y. Liu, K. Shimatake, T. Kurosawa, K. Ichimura, Y. Toda, M. Oda, and S. Tanda, *Phys. Rev. Lett.* **105**, 176401 (2010).
- [11] C. Monney, C. Battaglia, H. Cercellier, P. Aebi, and H. Beck, *Phys. Rev. Lett.* **106**, 106404 (2011).
- [12] H. Hughes, *J. Phys. C: Solid State Physics* **10**, L319 (1977).
- [13] M. H. Whangbo and E. Canadell, *J. Am. Chem. Soc.* **114**, 9587 (1992).
- [14] J. van Wezel, P. Nahai-Williamson, and S. S. Saxena, *Phys. Rev. B* **81**, 165109 (2010).
- [15] B. Zenker, H. Fehske, H. Beck, C. Monney, and A. Bishop, *Physical Review B* **88**, 075138 (2013).
- [16] C. Lian, Z. A. Ali, and B. M. Wong, *Phys. Rev. B* **100**, 205423 (2019).
- [17] E. Baldini, A. Zong, D. Choi, C. Lee, M. H. Michael, L. Windgatter, I. I. Mazin, S. Latini, D. Azoury, B. Lv, et al., *arXiv preprint arXiv:2007.02909* (2020).
- [18] D. Lioi, R. Schaller, G. Wiederrecht, and G. Karapetrov, *arXiv preprint arXiv:1612.01838* (2016).
- [19] E. Möhr-Vorobeva, S. L. Johnson, P. Beaud, U. Staub, R. De Souza, C. Milne, G. Ingold, J. Demsar, H. Schäfer, and A. Titov, *Phys. Rev. Lett.* **107**, 036403 (2011).
- [20] M. Burian, M. Porer, J. R. Mardegan, V. Esposito, S. Parchenko, B. Burganov, N. Gurung, M. Ramakrishnan, V. Scagnoli, H. Ueda, et al., *arXiv preprint arXiv:2006.13702* (2020).
- [21] P. B. Allen, *Phys. Rev. Lett.* **59**, 1460 (1987).
- [22] J. Sipe and A. Shkrebtii, *Physical Review B* **61**, 5337 (2000).
- [23] L. Keldysh and Y. V. Kopaev, *Soviet Physics Solid State, USSR* **6**, 2219 (1965).
- [24] D. Jérôme, T. Rice, and W. Kohn, *Phys. Rev.* **158**, 462 (1967).
- [25] G. Mazza, M. Rösner, L. Windgatter, S. Latini, H. Hübener, A. J. Millis, A. Rubio, and A. Georges, *Physical Review Letters* **124**, 197601 (2020).
- [26] R. Peierls, London, England p. 108 (1955).
- [27] W. T. B. Kelvin, *The molecular tactics of a crystal* (Clarendon Press, 1894).
- [28] F. J. Di Salvo, D. Moncton, and J. Waszczak, *Phys. Rev. B* **14**, 4321 (1976).
- [29] M. P. Silverman, *J. Opt. Soc. Am. A* **3**, 830 (1986).
- [30] See Supplemental Material at . . . for details on the computational methodology, approach to determine the degree of circular polarization from first principles and convergence tests of the structural phase transition using different approximations within DFT.
- [31] T. Buslaps, R. Johnson, and G. Jungk, *Thin Solid Films* **234**, 549 (1993).
- [32] S. Bayliss and W. Liang, *Journal of Physics C: Solid State Physics* **18**, 3327 (1985).
- [33] K. Velebit, P. Popčević, I. Batistić, M. Eichler, H. Berger, L. Forró, M. Dressel, N. Barišić, and E. Tutiš, *Phys. Rev. B* **94**, 075105 (2016).
- [34] Y. I. Joe, X. Chen, P. Ghaemi, K. Finkelstein, G. de La Peña, Y. Gan, J. Lee, S. Yuan, J. Geck, G. MacDougall, et al., *Nature Physics* **10**, 421 (2014).
- [35] A. Wegner, D. Louca, and J. Yang, *Phys. Rev. B* **99**, 205110 (2019).
- [36] A. Wegner, J. Zhao, J. Li, J. Yang, A. Anikin, G. Karapetrov, K. Esfarjani, D. Louca, and U. Chatterjee, *Phys. Rev. B* **101**, 195145 (2020).
- [37] M. D. Watson, A. M. Beales, and P. D. King, *Phys. Rev. B* **99**, 195142 (2019).
- [38] J. M. Moya, C.-L. Huang, J. Choe, G. Costin, M. S. Foster, and E. Morosan, *Phys. Rev. Mat.* **3**, 084005 (2019).
- [39] D. J. Campbell, C. Eckberg, P. Y. Zavalij, H.-H. Kung, E. Razzoli, M. Michiardi, C. Jozwiak, A. Bostwick, E. Rotenberg, A. Damascelli, et al., *Phys. Rev. Mat.* **3**, 053402 (2019).
- [40] C. Oglesby, E. Bucher, C. Kloc, and H. Hohl, *Journal of crystal growth* **137**, 289 (1994).
- [41] P. E. Blöchl, *Phys. Rev. B* **50**, 17953 (1994).
- [42] G. Kresse and J. Hafner, *Phys. Rev. B* **47**, 558 (1993).
- [43] G. Kresse and J. Furthmüller, *Physical review B* **54**, 11169 (1996).
- [44] J. P. Perdew, K. Burke, and M. Ernzerhof, *Phys. Rev. Lett.* **77**, 3865 (1996).
- [45] S. Grimme, J. Antony, S. Ehrlich, and H. Krieg, *J. Chem. Phys.* **132**, 154104 (2010).
- [46] A. Togo and I. Tanaka, *arXiv preprint arXiv:1808.01590* (2018).